

Accepted Manuscript

Carbonization of biomass: Effect of additives on alkali metals residue, SO₂ and NO emission of chars during combustion

Jianhui Qi, Kuihua Han, Qian Wang, Jie Gao

PII: S0360-5442(17)30675-8

DOI: [10.1016/j.energy.2017.04.109](https://doi.org/10.1016/j.energy.2017.04.109)

Reference: EGY 10750

To appear in: *Energy*

Received Date: 2 December 2016

Revised Date: 19 April 2017

Accepted Date: 20 April 2017

Please cite this article as: Qi J, Han K, Wang Q, Gao J, Carbonization of biomass: Effect of additives on alkali metals residue, SO₂ and NO emission of chars during combustion, *Energy* (2017), doi: 10.1016/j.energy.2017.04.109.

This is a PDF file of an unedited manuscript that has been accepted for publication. As a service to our customers we are providing this early version of the manuscript. The manuscript will undergo copyediting, typesetting, and review of the resulting proof before it is published in its final form. Please note that during the production process errors may be discovered which could affect the content, and all legal disclaimers that apply to the journal pertain.



Carbonization of biomass: effect of additives on alkali metals residue, SO₂ and NO emission of chars during combustion

Jianhui Qi^{a,b}, Kuihua Han^{a,*}, Qian Wang^a, Jie Gao^a

^a*School of Energy and Power Engineering, Shandong University, Jinan 250061, China*

^b*School of Mechanical and Mining Engineering, The University of Queensland, Brisbane QLD 4072, Australia*

Abstract

The effect of additives (NH₄H₂PO₄, CaCO₃ and CaO) on biomass carbonization was studied in the current paper, including residual K and Na in chars, SO₂ and NO emission of different chars during combustion. Experiment was carried on a tube furnace system. The results show that, CaO and NH₄H₂PO₄ reduce the alkali content of chars to different degree. Three additives inhibit SO₂ emission from raw and carbonized biomass remarkably, and SO₂ mass emission is lesser than 0.1 mg g⁻¹. Three additives enhance NO emission at different levels, and NO mass emission is from 1.2 to 3.5 mg g⁻¹. Both raw and carbonized biomass can be modified by some additives to achieve near zero emissions of SO₂. Although the additives promote the NO release, the total emission rate (3.8 to 10.1 %) was much lower than that of brown coal combustion, which was reported as 33.5 to 37.7 %. Economic analysis shows that three additives are economy for industry utility. Thus the three additives are good for modifying biomass carbon to attain clean and efficient combustion.

Keywords: Biomass carbonization, alkali metal, SO₂, NO, additive

*Corresponding author

Email address: hankh@163.com (Kuihua Han)

1. Introduction

Biomass, a type of renewable energy resource[1, 2], can be basically divided into various types, namely woody plants, herbaceous plants, aquatic plants, manures, municipal solid waste (MSW), organic waste/residue. Generally, biomass can be converted into three main types of product, electrical/heat energy, transport fuel, chemical feedstock[3, 4, 5, 6, 7, 8, 9]. In China, as reported by the twelfth Five-Year-Plan for biomass energy development[10], potential biomass resource consist of 37% of crop straw, 43% of wood waste and 20% of other organic waste/residue, is equal to totaling 460 million tons standard coal per annum.

In 2016, the ratio of renewable energy consumption to the total energy consumption was 11.64%, and the biomass energy took into account only 8.00% of total renewable energy. As reported by the China's thirteenth Five-Year-Plan for biomass energy development[11], the biomass energy utility will reach to 57 million tons of standard coal. Obviously, there is a huge space of biomass utilization. In order to achieve extensive utilization and higher efficiency, it is urgent to develop technologies about upgrading and pretreatment of multifarious biomass resource in China.

There are multiple ways for upgrading biomass fuels, such like densifying and molding, which have already been widely used[12, 13, 14]. Alternatively, torrefaction, carbonization, pyrolysis and gasification are more effective ways to upgrade biomass than densifying and molding, especially for crop straws which have lower energy density than the ordinary coal. Torrefaction is a thermal pre-treatment process for biomass at temperature range of 200 to 300 °C in an inert atmosphere[15]. Carbonization is a process that operated at temperatures of 300 to 500 °C with an inert atmosphere to obtain highly fragrant refractory solid matter[16, 17]. **Pyrolysis is a thermal process that heats and decomposes biomass at high temperature** (300 to 1000 °C)[18, 19, 20, 21, 22, 23, 24] in an inert environment while gasification is a promising method to produce "product gas" with lower temperature (below 1000 °C) and "syngas" with high temperature (above 1200 °C)[25]. Among them, torrefied or carbonized biomass shows potential performance on combustion, co-combustion with coal or gasification[26, 27], which has higher energy density, good grindability and combustion characteristics[28].

Remarkably, higher content of chlorine (Cl) and alkali metals (potassium K and sodium Na) in biomass, like high-potassium crops straw and stalk, comes with in grave ash deposition, slagging in both circulating fluidized

bed and grate furnaces[29, 30, 31, 32], and bed agglomeration of fluidized-bed gasification[33]. Similarly, the residual alkali metals in chars of biomass carbonization are also worth studying, which affect its utilization as an alternative solid fuel for the aforementioned aspects. Little work has been done on ash fusibility of torrefied or carbonized biomass, especially potassium-rich crops straw and stalk. Investigation of ash fusibility and transformation of alkali metals of biomass in co-gasification, co-combustion process[34, 35, 36, 37, 38] provides significant hints for improving the ash fusibility, mainly involving the conversion of alkali metals to high melting point compounds: KAlSi_2O_6 (1500 °C), CaKPO_4 (1560 °C), $\text{Ca}_2\text{Al}_2\text{SiO}_7$ (1593 °C), $\text{K}_2\text{Ca}(\text{SiO}_4)_2$ (1600 °C), $\text{Na}_2\text{Al}_2\text{Si}_2\text{O}_8$ (1250 °C), $\text{CaK}_2\text{P}_2\text{O}_7$ (1143 °C), etc.

Although the sulfur content of biomass is much little, and the nitrogen content is close to that of coal, the emission standards of flue gas pollutants of biomass fired boilers still become stricter. In China, the emission standards of flue gas pollutants of biomass fired boilers in demonstration projects (i.e. the thermal capacity of single boiler is above 7 MW), were issued in July 2014 by National Energy Administration and Ministry of Environmental Protection of PRC, limiting dust emission concentration of 30 mg m^{-3} , SO_2 emission concentration of 50 mg m^{-3} , and NO_x emission concentration 200 mg m^{-3} (standard condition: temperature of 273 K, pressure of 101 325 Pa, dry flue gas). Therefore, it is necessary to develop appropriate technology for clean and efficient utilization of biomass. Many studies[39, 40, 41, 42, 43, 44, 45, 46, 47] reported that the SO_2 and NO_x emission reduces during biomass combustion or co-combustion with coal. However, few study focuses on combustion characteristics and SO_2 and NO (main form of NO_x) emission of additives-loaded biomass chars obtained from different temperatures carbonization.

Calcium-based sorbents are generally used as sulfur retention additives for coal combustion, such as cheap and abundant limestone, the main composition of which is CaCO_3 . CaO , the main component of lime, is supposed to be higher active for locally desulfurization than CaCO_3 in high temperature carbonization and combustion process due to the following two reasons. Firstly, CaCO_3 is widely used as desulfurization additives[48, 49]. However, CaCO_3 should be decomposed into CaO first during high temperature (around 1100 °C), then the CaO will react with SO_2 or H_2S . Even though previous study[50] shows that the CaCO_3 may react with SO_2 directly, that will largely occurs only under the condition with high partial pressure of CO_2 . Secondly, the sulfur species, mainly SO_2 and H_2S , starting to significantly release by devolatilization at low temperature of around

300°C. During that temperature, the CaCO_3 is not significantly decomposed to CaO . Thus CaO is more active than the CaCO_3 . Moreover, lime is also proved suitable to reduce the sintering of biomass ash[51]. It was verified that phosphorus-rich additives, such as calcium phosphate ($\text{Ca}_3(\text{PO}_4)_2$), monocalcium phosphate ($\text{Ca}(\text{H}_2\text{PO}_4)_2$) and ammonium dihydrogen phosphate ($\text{NH}_4\text{H}_2\text{PO}_4$), are positive for capturing alkali metals, restraining the volatilization of alkali metals and inhibiting the sintering of ash during wheat straw combustion[52]. In the recent experimental study[53], through injecting powder of $\text{NH}_4\text{H}_2\text{PO}_4$ and KCl into the flue gas using drop tube furnace system, KCl can be effectively transformed into dipotassium hydrogen phosphate (K_2HPO_4), potassium dihydrogen phosphate (KH_2PO_4), potassium metaphosphate ($(\text{KPO}_3)_n$), potassium pyrophosphate ($\text{K}_4\text{P}_2\text{O}_7$), potassium ammonium phosphate and potassium-ammonium dihydrogen phosphate when the reactive temperature is in the range of 700 to 1000°C. Therefore, CaCO_3 , CaO and $\text{NH}_4\text{H}_2\text{PO}_4$ are selected as additives and expected to reduce SO_2 emission and ash sintering of alkali metal-rich biomass. Furthermore, these additives are the main composition/ionic compounds of some calcium-based industrial solid wastes, including red mud, carbide slag, white mud and phosphorus/nitrogen-rich sewage sludge, etc. Consequently, the performance of additives is supposed to offer meaningful suggestion for resource utilization of the calcium-based solid waste to modify biomass briquette fuel.

The objectives of this study are: (1) to explore the effect of three additives on the residual Na and K content of maize straw chars obtained from 300 to 800°C carbonization, (2) to explore the SO_2 and NO emission and conversion of additives-loaded/free raw biomass and their obtained chars. The results of this paper will contribute to modification, additives and clean combustion of carbonized biomass, the dust emission and flue gas cleaning.

2. Experimental Study

2.1. Property analysis of test samples

One of the herbaceous crops residue, namely maize straw (MS) was selected as the main biomass sample of this study. This is because maize is one of the most largest grown crops in north east China. It is cheap and convenient to acquire high quality MS biomass. Now the residue of MS is always used for biomass molding fuel, biomass heat and power generation, daily heating and cooking in this region. The MS sample used in this study were grown at rural areas in Dezhou, China. The raw MS, additive loaded

MS, carbonized MS, carbonized additive loaded MS samples were prepared by the following procedures.

In this study, the raw and carbonized biomass samples were all analyzed. The measurements include proximate, ultimate (elemental) analysis and calorific value measurement. The proximate and ultimate analysis were performed in accordance with the test methods for analysis of wood fuels of ASTM (American Society for Testing and Materials standard, E870-82(2013)) [54]. Specifically, the volatile content of the samples was analyzed with an auto volatile analyzer (CKIC 5E-MAG6600). The ultimate analysis was carried out using an ultimate analyzer (Leco TruSpec CHN) and sulfur analyzer (Leco S144DR). The higher heating values (HHVs) of the samples were measured by a bomb calorimeter (CKIC 5E-AC8018). The potassium (K) and sodium (Na) element contents were analyzed with a X-ray fluorescence (XRF) spectrometer (Tianrui WDX-200) and inductively coupled plasma-atomic emission spectrometry (ICP-AES, IRIS Advantage).

The property analysis of raw MS samples and the MS-chars are listed in Tab.1.

[Table 1 about here.]

2.2. Carbonization process

Before tests carried out, the received biomass was dried in an dryer at temperature of 105 °C for 20 h. Then the air dried MS biomass was ground into powders by a blade pulverizer. After that, the particle size of the MS biomass was selected between 85 and 200 mesh (i.e. 74 to 180 μm) with a vibrating screen sieve. The sieved biomass was dried again at 105 °C for 10 h to provide basic samples material for the following analysis and tests.

The additives, ammonium dihydrogen phosphate (ADP, $\text{NH}_4\text{H}_2\text{PO}_4$), calcium carbonate (CaCO_3) and calcium oxide (CaO) were made in Tianjin Kemiou Chemical Reagent Co., China and both were analytical pure. In previous study[55], a given K/P ratio of 1:1 was selected to be used as the benchmark for making the biomass additive mixture. Even in this study, both K and Na reaction ability would be studied, to make the study coherent, the same K to core reactive elements (P for ADP, Ca for CaCO_3 and CaO) ratio, i.e. 1:1, are selected to make the additive loaded MS sample. The sample mass and the additives mass based on this ratio for different samples are listed in Tab.2

[Table 2 about here.]

Then, the additive loaded MS samples were modified by those additives with soak (ADP), co-precipitation (CaCO_3) and mechanical blending (CaO) based on different chemical properties. For ADP loaded MS sample, MS raw biomass was mixed with ADP solution. The the mixture was stirred in electromagnetic agitator for 3 h, and dried in the drier at temperature of $105\text{ }^\circ\text{C}$ for 20 h, then grinded and dried again at $105\text{ }^\circ\text{C}$ for 10 h. In the similar way, the suspension liquid of CaCO_3 was used to modify the MS biomass. The grinded CaO powder was blended with MS biomass mechanically and stirred for 1 h, then dried again. However, the soak and co-precipitation methods were not recommended for practical processing for modifying biomass, biomass char or briquette solid fuel, due to the extra heating required to dry the extra moisture. They were used to get the best performance of additives during experiment. In practical, all the additives were recommended to be grinded and blended directly into the raw biomass.

[Figure 1 about here.]

The carbonization test system, as shown in Fig.1, was composed from a steel cylinder, a rotameter, a reactor and a product gas treatment unit. The steel cylinder was used to supply nitrogen for providing inert atmospheres. The volumetric flow rate of nitrogen was controlled by the rotameter. The reactor was composed from a corundum tube with sealing flanges and an electrical furnace. The diameter and the length of the corundum tube were 100 mm and 800 mm respectively, and the length of constant temperature zone was 200 mm, which was enough for the batch test on a alundum crucible. The flanges of both ends were connected to the nitrogen cylinder and conical flask was used to treat the product gas through a 10 mm mm air vent hole. Nitrogen entered into the tube from one side and was released through the conical flask following the carbonization of biomass samples. Following combustion, exhaust gas was cleaned with water filled in the conical flask to prevent pollutants entering the atmosphere. The electrical element of the furnace was composed of silicon carbide rods with rated power of 3 kW. The reaction temperature, from room temperature to $1500\text{ }^\circ\text{C}$, was controlled by a proportional integral derivative temperature controller while the coupling power for electric heating was controlled by a solid state relay power controller. Heating temperature profiles at various final temperatures of simulator for segmented heating carbonization furnace are shown in Fig.2. The size of the alumina boat was $120\times 60\times 20$ mm. When operating the furnace, the

alumina boat was placed at the middle of the thermostatic section to ensure precision of temperature measurement and an even heating. The samples were placed in the alumina boat for carbonization and the heater was used to elevate and sustain the reaction temperature.

[Figure 2 about here.]

In each test batch, the alumina containing test sample with a total mass of 10 g ($\pm 1\%$) was tiled as a 5 mm thin layer and put into the middle of thermostatic section of the corundum tube at each reaction temperature. The flanges were then tightened while the nitrogen supplied by the cylinder was introduced into the tube at a continuous flow rate of 2.0 L min^{-1} (25°C). Before heating, nitrogen was continuously blown into the reaction tube for 20 min to keep it in an inert environment. Then the electrical furnace was connected into power to heat the samples following the heating profile showing in Fig.2 in different temperature. Following this, heating was stopped and the furnace was left for cooling down naturally to 100°C with continuously nitrogen supplying. Finally, the alumina boat and sample were removed to a desiccator, cooled to room temperature and weighed. Each test mode was carried out three times to ensure accuracy. The results were fairly uniform between each patch and the relative error was less than 5%. After that, the carbonized products were stored in sample bottles for analysis.

2.3. SO_2 and NO emission studies

The SO_2 and NO emission experiment was conducted in the dual-tube combustion experimental system, as shown in Fig.3. The experimental device is made up of an air feeding system, a reaction system and a flue gas analyzer unit. The air cylinder provided a pressure stabilized supply of reaction air, which was aerated by an automatic air compressor periodically. The air came into the reaction system through the air pressure relief valve, and the volumetric air flow rate was controlled by the rotameter. The reaction system was composed of two corundum tubes which were connected by silicone tube with each other and an electrical furnace. The inner diameter and the length of the tube were 17 mm and 550 mm respectively. The upper corundum tube was acted as preheating section while the bottom one was acted as combustion tube. Air was supplied into the tubes from a 10 mm air vent hole which was traversed by quartz tube through the upper rubber plug. After preheated, the air kept going into the combustion tube to assist the

biomass combustion which happened in the constant temperature zone. The length of constant temperature zone was 150 mm, which was enough for alumina boat. The electronic furnace was composed of silicon carbide rods with electric heating power of 3 kW. The reaction temperature was controlled by a proportional integral derivative temperature controller, whereas the power of the heater was controlled by a solid state relay power controller.

[Figure 3 about here.]

For each test batch, the pulverized powder with a total mass of 100 ± 0.1 mg was evenly placed in an alumina boat ($77 \times 13 \times 9$ mm). When the temperature of tube was heated to 800 °C by the electrical furnace, the alumina boat was put into the middle of the thermostatic section of the combustion corundum tube. The rubber plug was then tightened while the air supplied by the cylinder was introduced into the tube at a continuous flow rate of 1 L min^{-1} (25 °C). During combustion, the exhaust flue gas was driven by a inter pump of the flue gas analyzer unit (MRU OPTIMA7) to pass through the filter and then analyzed by the flue gas analyzer. The flue gas component data was on-line acquired and processed by the computer. The air was continuously blown into the reaction tube for burnout of samples until the detected pollutant concentration decreased to near zero. Each test mode was usually carried three times. The results were fairly uniform between each patch and the relative error was less than 5 %.

In order to quantify the influence of additives on the carbonized biomass samples SO_2 and NO emission characters, four specific variables are defined. The total conversion of the S in samples (fuel-S) to SO_2 (V_S) and the total conversion of the N in samples (fuel-N) to NO (V_N) are described as

$$V_S = \frac{\int_{t_0}^t C_S(t)V(t)dt}{W_0 \cdot S_t} \cdot \frac{32}{64} \cdot 100 \quad (1)$$

$$V_N = \frac{\int_{t_0}^t C_N(t)V(t)dt}{W_0 \cdot N_t} \cdot \frac{14}{30} \cdot 100 \quad (2)$$

where t_0 is the initial time of experiment, s; t is a certain time during the experiment, s; $C_S(t)$ is the SO_2 concentration in flue gas corresponding to t , mg m^{-3} ; $C_N(t)$ is the NO concentration in flue gas corresponding to t , mg m^{-3} ; $V(t)$ is the flux of the flue gas which is kept at 1 L min^{-1}

$(1.5529 \times 10^{-5} \text{ m}^3 \text{ s}^{-1})$ during the experiment; W_0 is the mass of the tested sample, mg; S_t is the sulfur content of the tested sample, %; N_t is the nitrogen content of the tested sample, percent. They describe how much S or N escaping into gas phase from the solid phase.

The other two variables are mass emission of SO_2 (M_S) and NO (M_N), which are defined as the ratios of the total gaseous SO_2 and NO mass to the mass of the tested sample, respectively. The unit of which is mg g^{-1} , and defined as

$$M_S = V_S \cdot S_t \quad (3)$$

$$M_N = V_N \cdot N_t \quad (4)$$

Those variables are not only reflect the intensity of the emission but also reflect the content of S or N in the biomass samples.

3. Results and discussion

3.1. Effect of additives on residual Na and K element in char

Fig.4 shows the scatter-line plots which are presented the K and Na content of char and ratio of residual K and Na in char to raw MS. Fig.4 (a) and (b) report the K and Na content of the obtained char, which reflect the alkali metal features during following combustion. Fig.4 (c) and (d) show the amount of K and Na remained in the char, which indicate the influence of additives on the alkali metal transfer. It can be noticed from the Fig.4 (a) and (b) that the K and Na contents of char increase firstly and then decrease with increasing carbonization temperature. To explain this phenomenon, Fig.4 (c) and (d) should be analyzed first. It can be seen from Fig.4 (c) and (d) that the residual K and Na of both raw MS-Char and additives loaded char are decreasing with the increasing carbonization temperature. What's more, when the carbonization temperature is over 600°C , the decreasing speed of the ratio of residual K is increased. That is because, when the temperature is below 600°C , only a limited release of K and Na ($<10 \text{ wt} \%$) was observed[56, 57]. Once the temperature is higher than 600°C , the K and Na begin to release in big amount. More details for K releasing, the low temperature release of K was related to the thermal decomposition of alkaline carboxylates at approximately 300°C or of phenol-associated K at around 400°C [58]. This is because elemental K does not show a significant

sublimation at 500 °C, and starts sublimation around 700 °C[59]. It has been reported that K sublimation properties are governed by the reaction temperature during combustion and the content of chlorine in the samples. Biomass resources are not only rich in K but also rich in chlorine, which leads the K sublimation to start at approximately 700 °C as the phase of KCl before a completed dechlorination at 800 °C[56]. Above that temperature, the K sublimation phase is governed by thermal decomposition mechanism of K_2CO_3 while some other inorganic elements (e.g. Si, Ca, Al, S) also play significant roles in K retention. For Na, the releasing tendency is almost the same as K besides the starting temperature for largely releasing was around 400 °C[60].

[Figure 4 about here.]

Among those samples showed in Fig.4 (c) and (d), it can be seen that the ratio of residual K and Na of ADP loaded char samples has almost the same value and tendency of the raw MS char. $CaCO_3$ promotes the retention of K and Na into the char. In the opposite, CaO accelerates the K and Na releasing. That phenomena can be explained as following. Adding $CaCO_3$ enhances both the ratio of residual K and Na in the char, that is because, the carbonate dissociation will absorb the K to a ceramic phase, slow down the K release to the gas phase and compete with KCl and NaCl sublimation[57, 61]. However, when the temperature increasing, the release of K and Na after fully dechlorination is governed by the thermal decomposition of carbonates, leading to the release of K, KOH, Na and NaOH to the gas phase[56]. However, adding CaO leads the opposite process: the ratio of residual K and Na is decreasing with the increasing carbonization temperature. In other words, the CaO accelerates the K and Na releasing during the carbonization progress. As proposed by Johansen[57], the added CaO would occupy more anion, mainly Cl^- , especially in the reaction of higher temperature, which promoted the K^+ and Na^+ releasing during carbonization process. It has benefit for the promoting of alkali metal releasing during carbonization progress. If more alkali metal elements released during carbonization progress, less alkali metal elements would release during the combustion progress. Because for the application, carbonization process will happens in large factory, the released alkali metal elements will be handled centralized. Then the char occupies less alkali metal, which will be good for the following combustion utility.

The effect of ADP on the alkali metal elements is more complicated. As shown in Fig.4 (c) and (d), that the ratios of residual alkali metal elements in char are almost the same as raw MS char. If looking into detail, the ratio is slightly lower than MS char when the carbonization temperature lower than 600 °C for K and 400 °C for Na. That is because, when the carbonization temperature is lower than the critical temperature for large amount release of alkali metal element, ADP thermal decomposition will accelerate the volatile release, which the most volatile of biomass samples starting to released to the gas phase at 210 °C[62]. Those volatiles will carry some alkali metal elements. However, when the temperature is beyond the critical value, the polymerism effect[53] of ADP will retain the K or Na into the solid phase. Thus the ratio of residual K or Na is higher than the MS Char.

If looking back to Fig.4 (a) and (b), the initial content of K and Na is much lower than the others. That is because, the most volatile of biomass samples starting to released to the gas phase at 210 °C[62]. Due to the mass loss of volatile with the constant content of K and Na, there appears an increasing tendency for the content of alkali residual in biomass char before 600 °C for K and 400 °C for Na. Adding ADP and CaO before carbonization could reduce the final K and Na content in char. That is coincident with the tendency of ratio of residual alkali metal if considering the mass loss. Adding CaCO₃ will reduce the final alkali metal elements when the carbonization temperature is lower than 600 °C. However, it can be found that the effect on K and Na reducing for CaCO₃ is limited. The most obvious differences of K and Na contents between the additive-loaded MS samples and the original MS sample are 1.1 % and 1.0 % respectively. Thus, ADP and CaO loaded char will offer a better alkali metal releasing performance in the following combustion than the raw MS char and CaCO₃ loaded char.

3.2. SO₂ emission characteristics

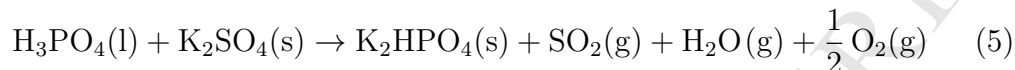
[Figure 5 about here.]

The SO₂ emission concentration of raw and modified MS, and the obtained additive loaded chars during combustion are reported in Fig.5. That the Fig.5 (a) is the SO₂ content of original MS sample and its obtained char samples during combustion. Fig.5 (b), (c) and (d) show the SO₂ content of raw MS with additive samples and their obtained char samples during combustion. It can be seen that there is only one large peak on the SO₂ release curves of raw and carbonized biomass combustion which is different from coal

combustion with two distinct release peaks[63, 64]. This can be explained by two reasons. One is the significant sulfur releasing (35 to 50% of the total S for herbaceous biomass) occurs during the initial devolatilization due to decomposition of organically associated sulfur in the fuels. The other one is that the sulfur released due to the decomposition of sulfate is retained in the char[65]. The MS with additives samples are reference samples during combustion. It can be noticed that, adding additives during raw MS combustion will reduce the SO₂ emission content dramatically compared to the raw MS combustion, which is from 97 mg m⁻³ for MS to 38, 67 and 39 mg m⁻³ for CaO, ADP and CaCO₃ loaded MS samples, which confirm the role of these additives on sulfur retention. If looking at the Fig.5 (a) that, although the sulfur content of the obtained char shows little changing with the increase of carbonization temperature, the SO₂ emission concentration still decreases from 97 mg m⁻³ to 54 mg m⁻³ and the starting point of SO₂ release delays with the reduction of volatiles within the obtained char. That indicates carbonization process could reduce the SO₂ emission content during the char combustion. What's more important is that the three additives, i.e. CaO, ADP (NH₄H₂PO₄) and CaCO₃, play a great role on sulfur retention during additive loaded char samples combustion. As shown in Fig.5 (b), (c) and (d), it could be seen that the maximum value of SO₂ emission content during additive loaded char samples are further reduced to 10, 43 and 37 mg m⁻³. CaO gets the best performance of sulfur emission during the char samples combustion. That is because, during carbonization CaO is active to react with S. Carbonization progress breaking the organic bond of S, then the S tends to react with Ca to generate CaS and CaSO₄, thus to reduce the organic S which can be transferred to SO₂ or SO₃ during the combustion. Due to that CaCO₃ will decompose under high temperature and transform to CaO, release CO₂, thus the reaction mechanism of CaCO₃ with S is much similar to the CaO. It can be inferred that the reaction of CaCO₃ with S happens after the decomposition reaction of CaCO₃ itself, so there is some S transferring other forms rather than the CaS or CaSO₄. During combustion, those part of sulfur release into the gas phase, that is why the content of SO₂ emission from CaCO₃ loaded char is higher than the CaO loaded char. CaO and CaCO₃ postpones the sulfur released from the decomposition of organic and inorganic sulfur in the char matrix with locally fixation. On the contrary, ADP promotes the sulfur release. It can be seen from the Fig.5 (c) that the release peak appears at about 60 s after the test.

That is because, during the carbonization progress, ADP initially accel-

erates dehydroxylation, prevent depolymerisation of samples to highly combustible tarry mixture[66, 67], and interrupt the bonds of organic sulfur. Moreover, during combustion progress, the inorganic metal sulfates, such as K_2SO_4 , can be converted by the following reactions to release SO_2 , especially for carbonized biomass modified by ADP.



Thus the SO_2 emission is ahead of schedule. However, ADP still acts good to prevent the SO_2 emission due to the polymer structure as shown in Fig.5 (c).

The SO_2 mass emission and conversion of raw and modified MS, and their char are presented in Fig.6. The hollow markers are the raw MS and raw MS with additives value. They are used as reference values here. The solid markers and lines represent obtained char samples.

[Figure 6 about here.]

It can be seen from the Fig.6 that the SO_2 mass emission M_S of raw MS was 0.57 mg g^{-1} corresponding to the conversion of fuel-S to SO_2 V_S of 10.83%. The SO_2 M_S of the obtained char for raw MS varies with the carbonization temperatures, as Fig.6 (a) showed, and achieves the maximum value of 0.97 mg g^{-1} corresponding to V_S of 18.9% at carbonization temperature of 500°C . It is interest that the M_S and V_S are going down first and then increasing to the maximum point at 500°C , after that point decreasing to the lowest value. That is due to the fact that when the carbonization temperature is set to around 400°C , the S release is faster than the locally fixation. However, as the carbonization temperature increasing, the locally fixation of S is faster than the S releasing into the gas phase. This change would be quite quick. That is the reason why there is a sharp turning corner on the Fig.6.

When the carbonization temperature is higher than 500°C , the locally fixation capacity for S of the char matrix is weakened due to the char matrix structure destroyed under the high carbonization temperature. Thus the M_S and the V_S are dropping with the increasing of carbonization temperature.

Three additives, ADP, CaO, $CaCO_3$ can inhibit the sulfur emission of all samples. As shown in the Fig.6, the SO_2 M_S for those samples are equal or less than 0.1 mg g^{-1} corresponding to V_S of less than 2.0%. It indicates

that the combustion process of the raw and carbonized biomass modified by additives can achieve near zero emissions of SO_2 .

The mechanism of sulfur retention or desulfurization by calcium based sorbent, including calcium carbonate (CaCO_3), calcium oxide (CaO), calcium acetate ($\text{Ca}(\text{CH}_3\text{COO})_2$), calcium propionate ($\text{C}_6\text{H}_{10}\text{CaO}_4$) etc., were studied in previous studies[63, 64]. They gave conclusions that, CaS and CaSO_4 were the production of CaO with H_2S and SO_2 corresponding in reducing and oxidizing atmosphere. Thus during the carbonization progress, S will be transform to CaS . Although ADP inspires the sulfur release early, it obtains similar performance for sulfur retention. It is resulting from the role of char during thermal conversion of biomass. As Knudsen et al.[65] indicated, the released sulfur is subsequently captured by reactive sites in the char matrix and become bound to the char. Sulfur presents as inorganic sulfate, e.g. K_2SO_4 , may partially react with char during devolatilization and become attached to the char matrix or transform to $\text{CaS}/\text{K}_2\text{S}$ depending on the carbonization temperature. During char burnout, inorganic sulfides and sulfur bounded to the char matrix are oxidized and released to the gas phase as SO_2 or transformed into solid CaSO_4 and K_2SO_4 . What is more important, the ADP has a significant effect on the microcosmic structure, changing from large particles with sever surface melting to mall, dispersed particles with rough and loose surface[55]. Those effect helps locally fixation of the S into the char matrix. And ADP can also improve the porosity of char during biomass pyrolysis [68, 69]. Thus the released sulfur can be more easily captured by the increased reactive sites in the char matrix and transformed to sulfur sulfates during the char burnout.

3.3. NO emission characteristics

NO emission concentration of raw and modified MS, and the obtained char are described in Fig.7 (a) to (d). Fig.7 (a) illustrates that, the release peak of NO for the raw MS is single, narrow and high, implying that the NO emission will occur at the beginning of the combustion stage, which is coincidence with the devolatilization peak of biomass. It can also be noticed that NO release peaks of the obtained MS char become broader with the increase of carbonization temperature, and the peak values decrease from 250 mg g^{-1} of raw MS to 80 mg g^{-1} of MS-800-char accordingly.

[Figure 7 about here.]

The conversion of fuel-N to NO of solid fuel are related with two sequential reaction steps corresponding to combustion of volatiles and char. Obviously the change is mainly attributable to the reduction of volatiles of the obtained char. From Fig.7 (b) to (d), the three additives diversely promote the production of NO for raw and carbonized MS. The peak values of raw and carbonized MS modified by additives significantly increase to different degrees, especially for samples modified by ADP. And the end points of NO release for the sample modified by ADP are prolonged simultaneously. That is because the amino from the ADP is decomposed with the ADP thermal composition and captured by the char matrix during the carbonization progress. Once burning the samples, the captured amino is released, oxidized and transformed to NO. In the mean time, the release amount of NO is also enhanced by CaO and CaCO₃ during the volatiles and char combustion stage, in accordance with Ca(CH₃COO)₂-loaded coal char and CaO-loaded coal combustion in literature[64, 70]. That significant phenomena was explained in those literature by regarding to the lack of stable organic component for N, which was more easier to be released during the following combustion stage than the S.

Fig.8 shows that the additives enhances the NO mass emission (M_N) and conversion (V_N) at different levels. As described above, the hollow markers represent the reference value, which are the M_N and V_N during raw MS and MS with additives. The solid markers and lines show the obtained chars value.

[Figure 8 about here.]

Comparing raw MS with MS char finds that the carbonization had little effect on the values of M_N and V_N , ranging from 1.22 to 1.61mg g⁻¹ and 3.83 to 6.42% respectively. But if looking at the additive loaded chars, the effect is more obvious, especially for the ADP loaded chars. The NO M_N and V_N are about twice bigger than those of additive free chars at various carbonization temperatures. The conversions of char N to NO increase with increasing carbonization temperatures both for pure char and the additives loaded chars. Similar results were obtained in Na/Fe/Ca/-loaded coal-char combustion by Zhao et al.[70]. This can be explained by two reasons. One reason is that calcium based compounds addition, such as Ca(OH)₂ and Ca(CH₃COO)₂, increases the amount of char N when the pyrolysis is performed in reduced circumstance[71]. It is also approved that NH₃ and HCN

are important intermediates for NO_x formation during nitrogen-containing solid fuel combustion. They undergo different oxidation mechanism and form different nitrogen oxides species. It is important to note that char-N increasingly plays a key role for NO production with reduction of volatiles content corresponding to increasing carbonization temperatures, as listed in Tab.1. The other reason is attributed to the loss of activity of char in NO-char reaction, which is known that both the oxidation of fuel-N to NO and the reduction of NO over char occurring simultaneously during char combustion.

Consequently, the NO emission level is determined by the effect on those two processes. The additives-loaded chars release more NO than the pure char, which suggests the additives enhances the conversion of char-N to NO[70]. Although the additives enhance the conversion of fuel-N to NO, the NO M_N is 1.2 to 3.5mg g^{-1} , and the conversion of 3.8 to 10.1% of the pure/additives-loaded MS-char is lower than 12.7 to 21.2% of the pure coal-char from pyrolysis reported in the literature[70], and much lower than 33.5 to 37.7% of brown coal combustion by similar experimental conditions in the literature[64]. It was proved[72] that biomass char made at lower pyrolysis temperature shows higher reactivity on NO reduction for larger specific surface area, comparing with coal-char. Considering that all the additives reduced the total emission (total amount of SO_2 , NO and alkali metal elements), which means the increased amount of NO is much less than the reduced amount of SO_2 and alkali metal elements, that those additives are helpful in reducing the pollution emission.

3.4. Economics analysis

Although the experimental results gave some beneficial enlightenment to improve biomass fuel by some additives, the rare mineral resources or high grade chemical products may undoubtedly show a low economic feasibility if they were used as additives of low-quality biomass briquette fuel. Based on the commercial cost of the additives and biomass fuel (mainly MS residual) in China, the prices of MS and additives are listed in Tab.3. Moreover, Tab.3 also list the amount of mass of additives required for modifying the MS. Then an approximate price increasing percent could be calculated. If ammonium dihydrogen phosphate ($\text{NH}_4\text{H}_2\text{PO}_4$), lime (CaO) and limestone (CaCO_3), are used in raising grade of biomass fuels, the producing cost will approximately increase by around 7.2 %, 1.5% and 2.1% corresponding to the Ca/K ratio of 1 and P/K ratio of 0.6 (slightly overdose), respectively.

Using calcium-based industrial solid waste and sewage sludge instead of mineral resources and chemical products will greatly reduce the cost of additives to modify biomass briquette fuel and disposal costs simultaneously. It is suggested that the effect of industrial solid waste on raw and carbonized biomass briquette fuel, such as ash fusibility, combustion performance and pollutant emission, should be further studied.

[Table 3 about here.]

4. Conclusions

Effect of additives ($\text{NH}_4\text{H}_2\text{PO}_4$, CaCO_3 and CaO) on biomass carbonization was studied, including the residual content of K and Na in chars and SO_2 and NO emission content of obtained chars during combustion. Results show that: (1) CaO and $\text{NH}_4\text{H}_2\text{PO}_4$ reduce alkali content of chars to different degree while CaCO_3 promotes the retention of alkali metal in the obtained char. (2) Carbonization reduces SO_2 emission during char combustion. Moreover, adding three additives during carbonization progress, SO_2 emission is further reduced during combustion. SO_2 mass emission of those additives loaded char samples less than 0.1 mg g^{-1} , which is almost zero. (3) Additives enhance the NO emission, and the NO mass emission is within the range of 1.2 to 3.5 mg g^{-1} . But those emission quantity is still under the limitation. (4) Those additives are helpful in reducing the pollution emission. (5) The three additives are economic and suitable for industry application.

5. Acknowledgments

This work was supported by Key Research and Development Program of Shandong Province (2016GGX104005), Interdisciplinary Development Program of Shandong University (2016JC005) and National Natural Science Foundation of China (51206096). The author, Jianhui Qi, will thank for the support of CSC (China Scholarship Council). Thanks Dr. Suoying He for the proofreading.

- [1] G. Boyle, et al., Renewable energy: power for a sustainable future, Taylor & Francis, 1997.
- [2] J. Qi, T. Reddell, K. Qin, K. Hooman, I. H. Jahn, Journal of Turbomachinery 139 (2017) 081008.1–081008.11.

- [3] N. L. Ma, K. Y. Teh, S. S. Lam, A. M. Kaben, T. San Cha, *Bioresource technology* 190 (2015) 536–542.
- [4] Q. Wang, K. Han, J. Gao, H. Li, C. Lu, *Fuel* 199 (2017) 488–496.
- [5] Q. Wang, K. Han, J. Gao, J. Wang, C.-m. Lu, *Energy & Fuels* (2017).
- [6] S. S. Lam, R. K. Liew, X. Y. Lim, F. N. Ani, A. Jusoh, *International Biodeterioration & Biodegradation* 113 (2016) 325–333.
- [7] S. S. Lam, W. A. W. Mahari, C. K. Cheng, R. Omar, C. T. Chong, H. A. Chase, *Energy* 115 (2016) 791–799.
- [8] S. S. Lam, H. A. Chase, *Energies* 5 (2012) 4209–4232.
- [9] N. L. Ma, Z. Rahmat, S. S. Lam, *International journal of molecular sciences* 14 (2013) 7515–7541.
- [10] Biomass Energy Development Plan for China Twelfth Five-Year-Plan, Technical Report, National Energy Administration of People’s Republic of China, 2011.
- [11] Biomass Energy Development Plan for China Thirteenth Five-Year-Plan, Technical Report, National Energy Administration of People’s Republic of China, 2016.
- [12] A. E. Ray, C. Li, V. S. Thompson, D. L. Daubaras, N. J. Nagle, D. S. Hartley, in: *Biomass Volume Estimation and Valorization for Energy*, InTech, 2017.
- [13] M. Soleimani, X. L. Tabil, R. Grewal, L. G. Tabil, *Fuel* 193 (2017) 134–141.
- [14] R. Tabakaev, I. Shanenkov, A. Kazakov, A. Zavorin, *Journal of Analytical and Applied Pyrolysis* (2017).
- [15] K. M. Sabil, M. A. Aziz, B. Lal, Y. Uemura, *Applied energy* 111 (2013) 821–826.
- [16] H. Abdullah, H. Wu, *Energy & Fuels* 23 (2009) 4174–4181.
- [17] H. Wu, M. N. Pedersen, J. B. Jespersen, M. Aho, J. Roppo, F. J. Frandsen, P. Glarborg, *Energy & Fuels* 28 (2013) 199–207.

- [18] S. S. Lam, R. K. Liew, A. Jusoh, C. T. Chong, F. N. Ani, H. A. Chase, *Renewable and Sustainable Energy Reviews* 53 (2016) 741–753.
- [19] S. S. Lam, R. K. Liew, C. K. Cheng, H. A. Chase, *Applied Catalysis B: Environmental* 176 (2015) 601–617.
- [20] W. A. Wan Mahari, N. F. Zainuddin, W. M. N. Wan Nik, C. T. Chong, S. S. Lam, *Energies* 9 (2016) 780.
- [21] A. D. Russell, E. I. Antreou, S. S. Lam, C. Ludlow-Palafox, H. A. Chase, *RSC Advances* 2 (2012) 6756–6760.
- [22] S. S. Lam, A. D. Russell, H. A. Chase, *Industrial & Engineering Chemistry Research* 49 (2010) 10845–10851.
- [23] S. S. Lam, W. A. W. Mahari, A. Jusoh, C. T. Chong, C. L. Lee, H. A. Chase, *Journal of Cleaner Production* 147 (2017) 263–272.
- [24] S. S. Lam, R. K. Liew, Y. M. Wong, E. Azwar, A. Jusoh, R. Wahi, *Waste and Biomass Valorization* (2016) 1–11.
- [25] N. A. Samiran, M. N. M. Jaafar, J.-H. Ng, S. S. Lam, C. T. Chong, *Renewable and Sustainable Energy Reviews* 62 (2016) 1047–1062.
- [26] S.-W. Du, W.-H. Chen, J. A. Lucas, *Bioresource technology* 161 (2014) 333–339.
- [27] A. T. Wijayanta, M. S. Alam, K. Nakaso, J. Fukai, K. Kunitomo, M. Shimizu, *Fuel Processing Technology* 117 (2014) 53–59.
- [28] M. Van der Stelt, H. Gerhauser, J. Kiel, K. Ptasinski, *Biomass and bioenergy* 35 (2011) 3748–3762.
- [29] A.-L. Elled, K. Davidsson, L.-E. Åmand, *Biomass and bioenergy* 34 (2010) 1546–1554.
- [30] L. Li, C. Yu, F. Huang, J. Bai, M. Fang, Z. Luo, *Energy & Fuels* 26 (2012) 6008–6014.
- [31] Y. Niu, Y. Zhu, H. Tan, S. Hui, Z. Jing, W. Xu, *Fuel Processing Technology* 128 (2014) 499–508.

- [32] H. Zhou, B. Zhou, H. Zhang, L. Li, K. Cen, *Industrial & Engineering Chemistry Research* 53 (2014) 7233–7246.
- [33] X. Wei, U. Schnell, K. R. Hein, *Fuel* 84 (2005) 841–848.
- [34] B.-M. Steenari, A. Lundberg, H. Pettersson, M. Wilewska-Bien, D. Andersson, *Energy & Fuels* 23 (2009) 5655–5662.
- [35] L. Li, Q. Ren, S. Li, Q. Lu, *Energy & Fuels* 27 (2013) 5923–5930.
- [36] L. Wang, G. Skjevrak, J. E. Hustad, Ø. Skreiberg, *Energy & Fuels* 28 (2013) 208–218.
- [37] T. Yang, J. Ma, R. Li, X. Kai, F. Liu, Y. Sun, L. Pei, *Energy & Fuels* 28 (2014) 3096–3101.
- [38] R. Li, X. Kai, T. Yang, Y. Sun, Y. He, S. Shen, *Energy Conversion and Management* 83 (2014) 197–202.
- [39] K. J. Wolf, A. Smeda, M. Müller, K. Hilpert, *Energy & fuels* 19 (2005) 820–824.
- [40] Z. Li, W. Zhao, R. Li, Z. Wang, Y. Li, G. Zhao, *Bioresource technology* 100 (2009) 2278–2283.
- [41] J. Bai, C. Yu, L. Li, P. Wu, Z. Luo, M. Ni, *Energy & Fuels* 27 (2012) 515–522.
- [42] J. Krzywański, R. Rajczyk, W. Nowak, *Chemical and Process Engineering* 35 (2014) 217–231.
- [43] J. Krzywanski, T. Czakiert, A. Blaszcuk, R. Rajczyk, W. Muskala, W. Nowak, *Fuel Processing Technology* 139 (2015) 73–85.
- [44] J. Krzywanski, W. Nowak, *Journal of Energy Engineering* 142 (2015) 04015017.
- [45] P. Basu, *Biomass gasification, pyrolysis and torrefaction: practical design and theory*, Academic press, 2013.
- [46] J. H. Miedema, R. M. Benders, H. C. Moll, F. Pierie, *Applied Energy* 187 (2017) 873–885.

- [47] S. Zhang, X. Jiang, B. Liu, G. Lv, Y. Jin, J. Yan, *Energy & Fuels* (2017).
- [48] C. Furnas, *Industrial & Engineering Chemistry* 23 (1931) 534–538.
- [49] T. Rajeswara Rao, *The Canadian Journal of Chemical Engineering* 71 (1993) 481–484.
- [50] C. Tullin, E. Ljungstroem, *Energy & Fuels* 3 (1989) 284–287.
- [51] M. F. Llorente, P. D. Arocas, L. G. Nebot, J. C. García, *Fuel* 87 (2008) 2651–2658.
- [52] L. Li, Q. Ren, S. Li, Q. Lu, *CSEE proceedings* 33 (2013) 41–47.
- [53] K. Han, J. Qi, H. Li, C. Lu, *CIESC Journal* 65 (2014) 1093–1098.
- [54] A. International, ASTM standard E870-82. standard test methods for analysis of wood fuels, 2013.
- [55] J. Qi, H. Li, K. Han, Q. Zuo, J. Gao, Q. Wang, C. Lu, *Energy* 102 (2016) 244–251.
- [56] J. N. Knudsen, P. A. Jensen, K. Dam-Johansen, *Energy & Fuels* 18 (2004) 1385–1399.
- [57] J. M. Johansen, J. G. Jakobsen, F. J. Frandsen, P. Glarborg, *Energy & Fuels* 25 (2011) 4961–4971.
- [58] S. C. van Lith, P. A. Jensen, F. J. Frandsen, P. Glarborg, *Energy & Fuels* 22 (2008) 1598–1609.
- [59] D. Bapat, S. Kulkarni, V. Bhandarkar, Design and operating experience on fluidized bed boiler burning biomass fuels with high alkali ash, Technical Report, American Society of Mechanical Engineers, New York, NY (United States), 1997.
- [60] K. Davidsson, J. Korsgren, J. Pettersson, U. Jäglid, *Fuel* 81 (2002) 137–142.
- [61] A. Novakovic, S. C. van Lith, F. J. Frandsen, P. A. Jensen, L. B. Holgersen, *Energy & Fuels* 23 (2009) 3423–3428.
- [62] E. Biagini, F. Lippi, L. Petarca, L. Tognotti, *Fuel* 81 (2002) 1041–1050.

- [63] J. Cheng, J. Zhou, J. Liu, Z. Zhou, Z. Huang, X. Cao, X. Zhao, K. Cen, *Progress in Energy and Combustion Science* 29 (2003) 381–405.
- [64] S. Niu, K. Han, C. Lu, *Chemical engineering journal* 168 (2011) 255–261.
- [65] J. N. Knudsen, P. A. Jensen, W. Lin, F. J. Frandsen, K. Dam-Johansen, *Energy & Fuels* 18 (2004) 810–819.
- [66] J. Xu, M. Gao, H. Guo, X. Liu, Z. Li, H. Wang, C. Tian, *Journal of fire sciences* 20 (2002) 227–235.
- [67] M. GAO, S. Li, C. Sun, *Combustion science and technology* 176 (2004) 2057–2070.
- [68] T.-H. Liou, *Chemical Engineering Journal* 158 (2010) 129–142.
- [69] W. C. Lim, C. Srinivasakannan, N. Balasubramanian, *Journal of Analytical and Applied Pyrolysis* 88 (2010) 181–186.
- [70] Z. Zhao, W. Li, J. Qiu, B. Li, *Fuel* 82 (2003) 1839–1844.
- [71] Y. Gu, X. Liu, B. Zhao, W. Liu, M. Xu, *Asia-Pacific Journal of Chemical Engineering* 8 (2013) 567–577.
- [72] L. Dong, S. Gao, W. Song, G. Xu, *Fuel Processing Technology* 88 (2007) 707–715.

List of Figures

1	Schematic diagram of carbonization tube furnace experiment system.	24
2	Heating temperature profiles of carbonization experiments. . .	25
3	Schematic diagram of the SO ₂ and NO emission experiment system	26
4	Change of (a)K content, (b)Na content, (c)ratio of residual K of char and (d)ratio of residual Na of char for MS carbonization	27
5	SO ₂ concentration for (a)MS and chars, (b)CaO-loaded MS and Chars, (c)ADP-loaded MS and chars, and (d)CaCO ₃ -loaded MS and chars	28
6	SO ₂ mass emission and conversion for modified MS, and their char. (a)SO ₂ mass emission, (b)SO ₂ conversion from fuel-S . .	29
7	NO concentration for (a)MS and chars, (b)CaO-loaded MS and Chars, (c)ADP-loaded MS and chars, and (d)CaCO ₃ -loaded MS and chars	30
8	NO concentration for (a)MS and chars, (b)CaO-loaded MS and Chars, (c)ADP-loaded MS and chars, and (d)CaCO ₃ -loaded MS and chars	31

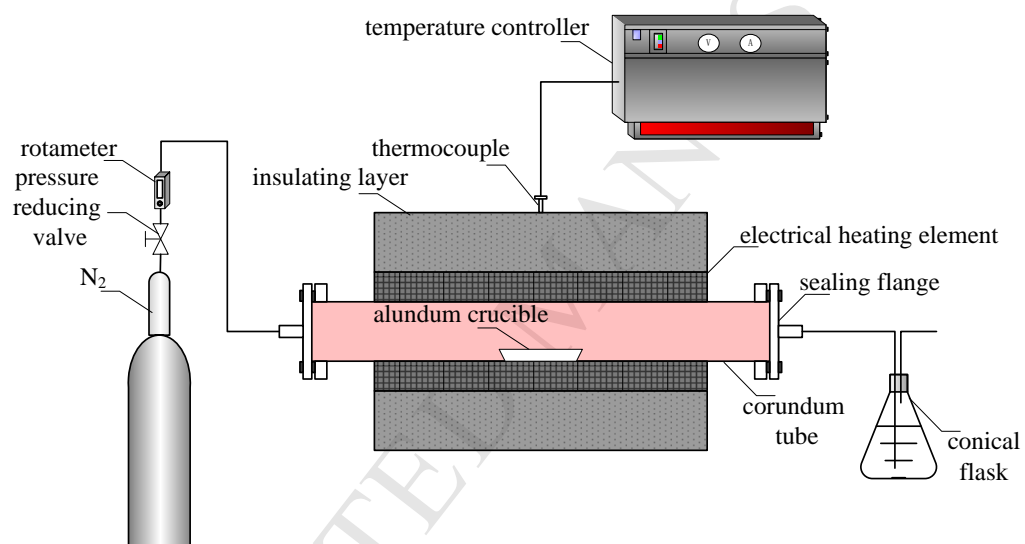


Figure 1: Schematic diagram of carbonization tube furnace experiment system.

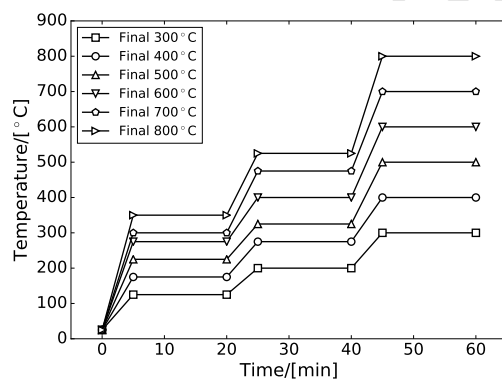


Figure 2: Heating temperature profiles of carbonization experiments.

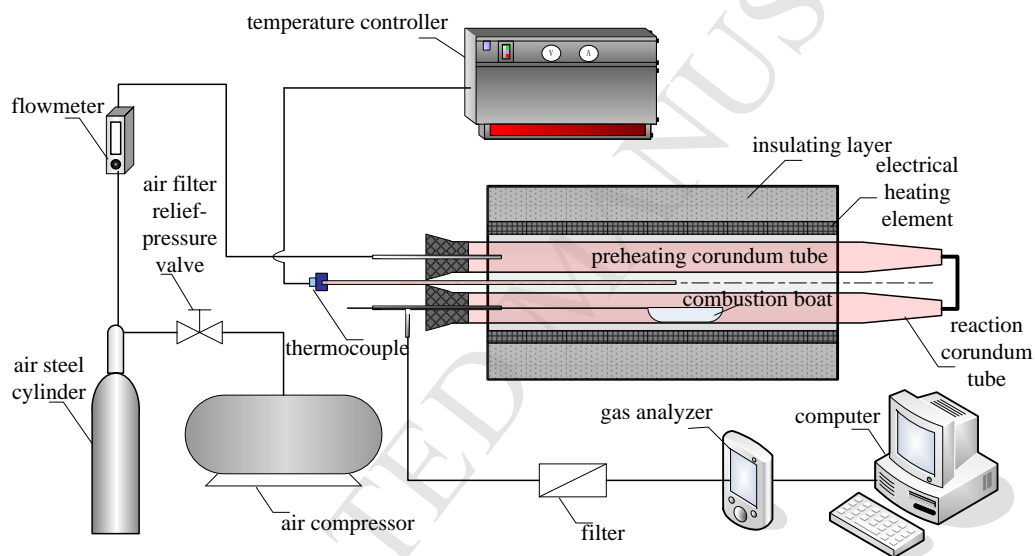


Figure 3: Schematic diagram of the SO₂ and NO emission experiment system

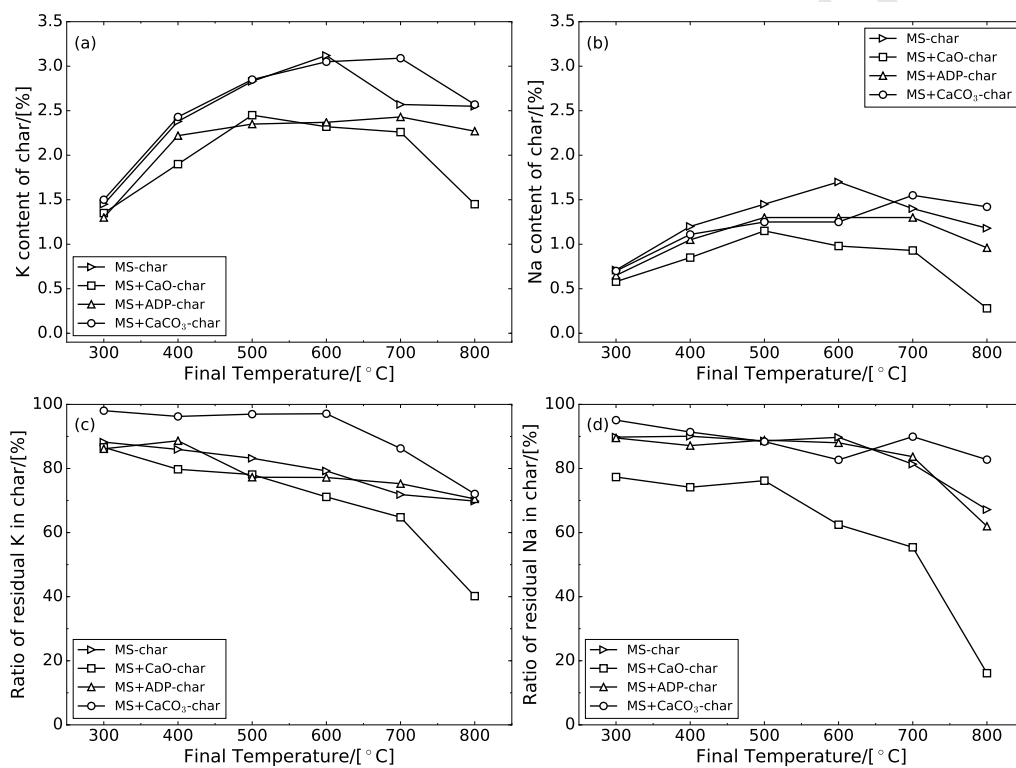


Figure 4: Change of (a)K content, (b)Na content, (c)ratio of residual K of char and (d)ratio of residual Na of char for MS carbonization

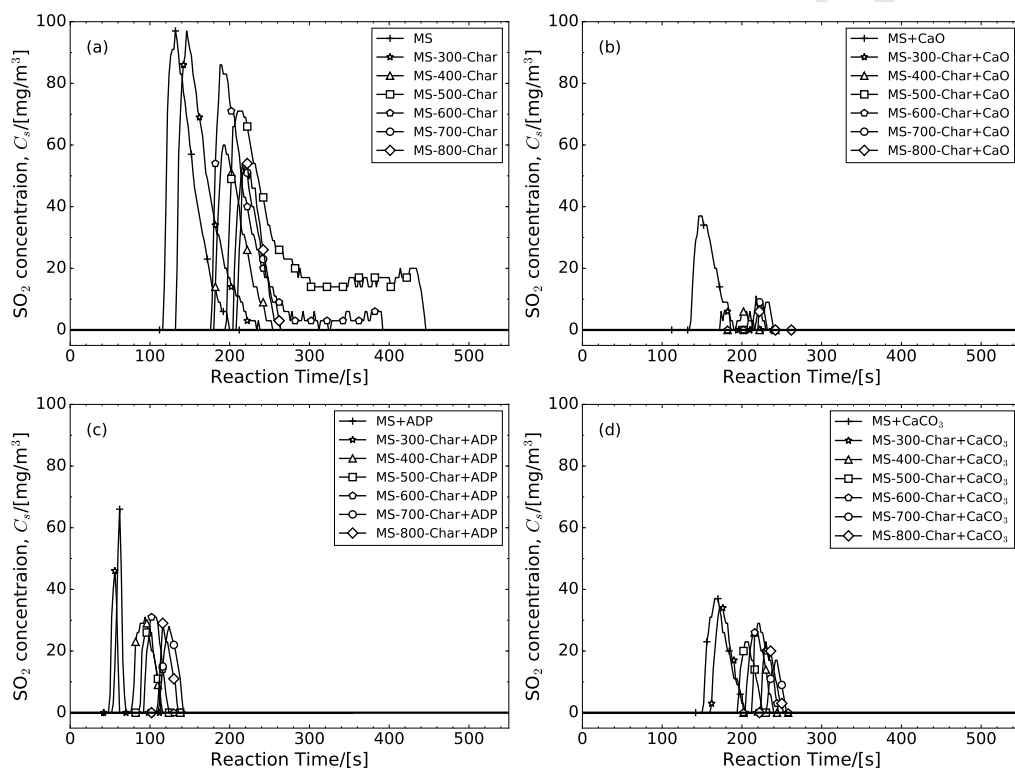


Figure 5: SO₂ concentration for (a)MS and chars, (b)CaO-loaded MS and Chars, (c)ADP-loaded MS and chars, and (d)CaCO₃-loaded MS and chars

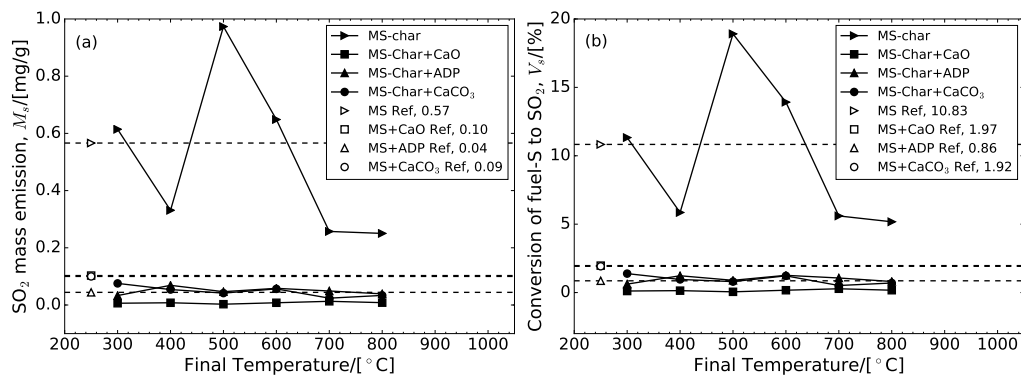


Figure 6: SO₂ mass emission and conversion for modified MS, and their char.
 (a)SO₂ mass emission, (b)SO₂ conversion from fuel-S

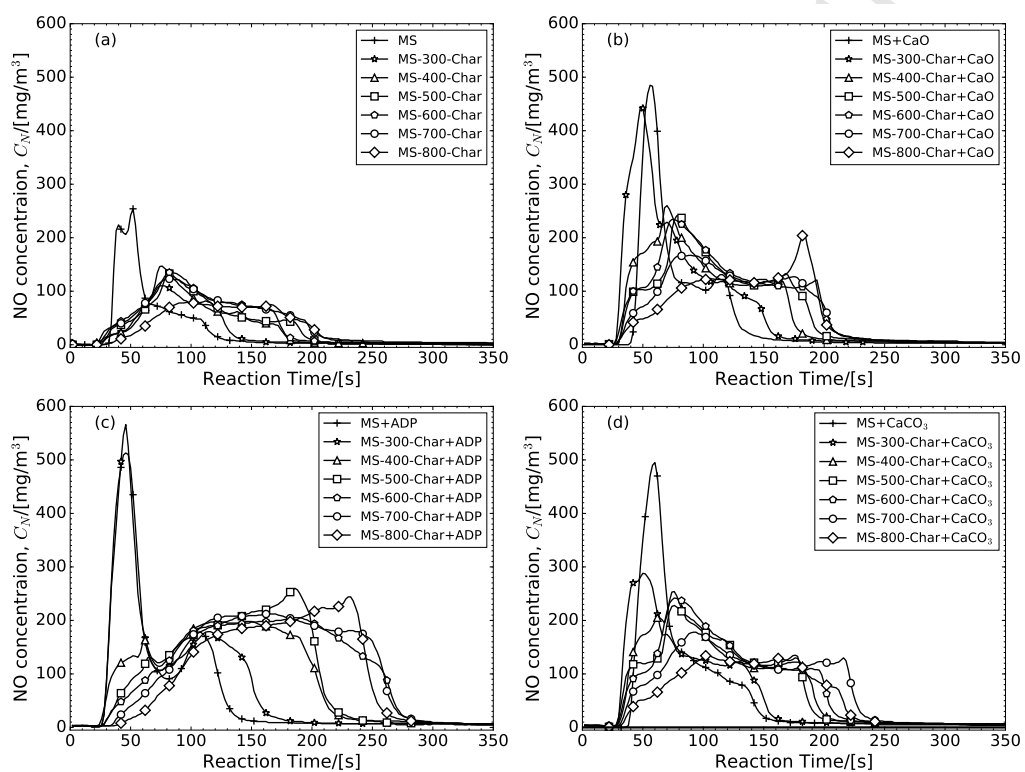


Figure 7: NO concentration for (a)MS and chars, (b)CaO-loaded MS and Chars, (c)ADP-loaded MS and chars, and (d)CaCO₃-loaded MS and chars

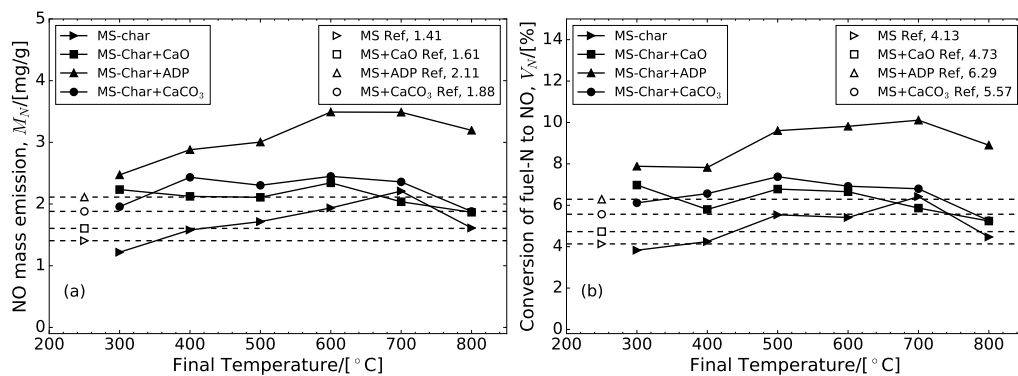


Figure 8: NO concentration for (a)MS and chars, (b)CaO-loaded MS and Chars, (c)ADP-loaded MS and chars, and (d)CaCO₃-loaded MS and chars

List of Tables

1	Proximate analysis, ultimate analyses and heating values of MS (by weight. dry basis).	33
2	Mass of samples and additives.	34
3	The cost prices for three additives	35

ACCEPTED MANUSCRIPT

Table 1: Proximate analysis, ultimate analyses and heating values of MS (by weight. dry basis).

Samples	Proximate analysis (%)			Ultimate analyses (%)					Alkali metal (%)		Heating values (MJ/kg) HHVs ^d
	A ^a	V ^b	FC ^c	C	H	O	N	S	K	Na	
MS	7.67	75.66	16.67	47.03	7.01	36.34	1.68	0.28	1.06	0.51	19.02
MS-300-Char	11.00	63.15	25.84	52.32	5.75	29.13	1.52	0.28	1.45	0.71	21.50
MS-400-Char	18.29	37.06	44.65	58.29	4.50	16.84	1.79	0.29	2.38	1.20	22.12
MS-500-Char	25.52	22.81	51.67	56.02	3.58	13.06	1.54	0.27	2.83	1.45	23.04
MS-600-Char	26.13	18.80	55.08	58.40	2.99	10.51	1.74	0.24	3.12	1.70	23.85
MS-700-Char	24.24	12.15	63.61	66.51	2.71	4.62	1.68	0.24	2.57	1.40	25.12
MS-800-Char	24.04	8.94	67.02	67.93	2.23	3.80	1.75	0.25	2.55	1.18	25.37

^aA - Ash

^bV - Volatile

^cFC - Fixed Carbon

^dHHVs - Higher heating values

Table 2: Mass of samples and additives.

Samples	Based Mass(g)	K mass(g)	Additive mass(g)	Additive mass percent(%)
MS	10.0	0.106	0.000	0.00
MS+ADP	10.0	0.106	0.312	3.03
MS+CaO	10.0	0.106	0.152	1.50
MS+CaCO ₃	10.0	0.106	0.272	2.65

Table 3: The cost prices for three additives

	Price(CNY/t)	Price(USD/t)	Mass per ton of MS(t)	Price increasing percent(%)
MS	~500.0	~44.1	0.0	0.0
ADP	~2000.0	~514.7	0.018	7.2
CaO	~500.0	~73.5	0.015	1.5
CaCO ₃	~400.0	~58.8	0.027	2.1

Research Highlights:

- Effects of $\text{NH}_4\text{H}_2\text{PO}_4$, CaO and CaCO_3 on K, Na residual in biomass char are studied.
- Carbonation of biomass can enhance the combustion characteristic.
- Additives can help to get near zero SO_2 mission of chars during combustion.
- Additives will promote the NO **emission** of chars during combustion.
- Those Additives are economic for industry application.